Scars on quantum networks ignore the Lyapunov exponent

Holger Schanz and Tsampikos Kottos

Institut für Nichtlineare Dynamik, Universität Göttingen and Max-Planck-Institut für Strömungsforschung,
Bunsenstraße 10, D-37073 Göttingen, Germany

(Dated: February 8, 2008)

We show that enhanced wavefunction localization due to the presence of short unstable orbits and strong scarring can rely on completely different mechanisms. Specifically we find that in quantum networks the shortest and most stable orbits do not support visible scars, although they are responsible for enhanced localization in the majority of the eigenstates. Scarring orbits are selected by a criterion which does not involve the classical Lyapunov exponent. We obtain predictions for the energies of visible scars and the distributions of scarring strengths and inverse participation ratios.

One of the most striking ways in which the underlying classical dynamics of a chaotic system manifests itself in the corresponding quantum behavior is the *scar* phenomenon [1, 2, 3, 4, 5, 6, 7, 8, 9, 10]. A scar is a quantum eigenfunction with excess density near an unstable classical periodic orbit (PO). Such states are not expected within Random-Matrix Theory (RMT), which predicts that wavefunctions must be evenly distributed over phase space, up to quantum fluctuations [11]. Experimental evidence and applications of scars come from systems as diverse as microwave resonators [6], quantum wells in a magnetic field [7], Faraday waves in confined geometries [9], open quantum dots [8] and semiconductor diode lasers [10].

Quantum networks (graphs) are established models in the field of mesoscopic physics, from which most of the above examples are drawn, as well as in many other areas including molecular and mathematical physics and quantum computation (see [12, 13, 14, 15] and Refs. therein). In recent years they have become one of the most prominent tools in quantum chaos because they allow to study with simple means the applicability of RMT and its limitations due to system-specific properties [14, 15, 16]. For example, it was shown recently [5] that statistics of the bulk of graph eigenfunctions (including, e. g. the left eigenstate in Fig. 1a) conform with the existing theories describing the effect of short unstable periodic orbits on the localization properties of wavefunctions.

Therefore it is surprising that the same does not apply to the small but important group of strongly scarred eigenstates (Fig. 1a, right), which we study in this letter. We show that, contrary to common intuition and accepted theories [1, 2, 3, 4, 5], the shortest and least unstable orbits of the system produce almost no visible scars, although they are responsible for enhanced localization within the bulk of states. We derive a condition, Eq. (7) below, selecting orbits relevant for strong scarring from topological information only and without any reference to the classical Lyapunov exponent. Based on this insight we are able to give a criterion for the energies at which strong scars are to be expected, Eq. (9), and describe their statistical distribution, Eq. (12). In view of the numerous and diverse applications of quantum networks [12, 13, 14, 15, 16], these main results should be of broad interest in their own right. On top of this, some important conclusions generalize beyond graphs. In particular, our results provide clear evidence for the fact that *enhanced wavefunction localization due to the presence of short unstable orbits and strong scarring can in principle rely on completely unrelated mechanisms* and can also leave distinct traces in statistical measures such as the distribution of inverse participation ratios (IPR).

Following the quantization outlined in [14] we consider graphs which consist of V vertices connected by a set of B bonds. The number of bonds emanating from a vertex j is its valency v_j. A basis state on the network is specified by a *directed* bond $d = [i \rightarrow j]$, i. e. an ordered pair of connected vertices i, j. Hence a quantum wavefunction is just a set of $2B$ complex amplitudes a_d, normalized according to $\sum_d |a_d|^2 = 1$. The standard localization measure is the IPR

$$\mathcal{I} = \sum_{d=1}^{2B} |a_d|^4 \,. \tag{1}$$

Ergodic states which occupy each directed bond with the same probability have $\mathcal{I} = 1/2B$ and up to a constant factor depending on the presence of symmetries this is also the RMT prediction. In the other extreme $\mathcal{I} = 1$ indicates a state which is restricted to a single bond only, i. e. the greatest possible degree of localization.

Fig. 1b shows the distribution of $\mathcal{I}$ for fully connected graphs. Some features of this distribution are explained by the original scar theory of Heller [1] and extensions of it [2, 5]. The main idea is to connect localization properties of eigenfunctions to the dynamics of the system. For example, the identity $\langle \mathcal{I} \rangle = \lim_{T \rightarrow \infty} \frac{1}{T} \int_0^T \mathrm{d}t \, \langle P(t) \rangle$ expresses the mean IPR in terms of the quantum return probability (RP) $P(t)$, averaged over time and initial states. It is then argued that the short-time dynamics, approximated semiclassically with some short PO's, provides sufficient information for estimating $\langle \mathcal{I} \rangle$. Within
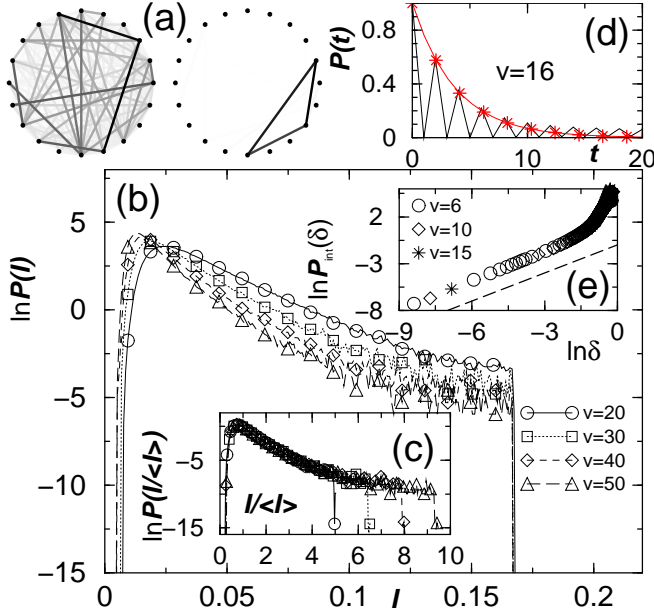
FIG. 1: Statistical properties of eigenstates for fully connected graphs with different valencies $v = V - 1$. The eigenstates were obtained by diagonalization of the bond-scattering matrix Eq. (4), and a statistical ensemble was generated by choosing random bond lengths. (a) The bond intensities of two representative eigenstates are shown with a gray-scale for a typical state (left) and a scar on a triangular PO (right). (b) Probability distribution of the IPR, showing a step-like cutoff at $\mathcal{I} = 1/6$ that can be attributed to scarring on triangular orbits. (c) The bulk of the IPR distribution shows scaling according to Eq. (2). (d) The quantum return probability and a classical approximation ($*$) based only on the period-two orbits; (e) Rescaled and integrated distribution of triangle scars $\mathcal{P}_{\text{int}}(\delta) = B^{-1} \int_0^\delta d\delta' \mathcal{P}^{(3)}(\delta')$. The dashed line has slope 1, corresponding to the theoretical prediction Eq. (12).

this approach it is clear that the orbits with the lowest Lyapunov exponent (LE) have the largest influence on eigenfunction localization because classical trajectories can cycle in their vicinity for a relatively long time and increase the RP beyond the ergodic average. For the graphs studied in this letter, some PO's p and their LE Λ_p are listed in Table I. The shortest PO's have period 2 and bounce back and forth between two vertices. For large graphs $v \to \infty$ these are by far the least unstable ones, as their LE approaches 0 while all others become increasingly unstable $\Lambda_p \sim \ln v$. Indeed the period 2 orbits totally dominate the classical and quantum RP at short times (see Fig. 1d). Including the contribution of these orbits only, Kaplan obtained a mean IPR which is by a factor $\sim v$ larger than the RMT expectation, in agreement with numerics [5]. Moreover, following the same line of argumentation as in [2] we get that the bulk of the IPR distribution scales as

$$\tilde{P}(\mathcal{I}/\langle \mathcal{I} \rangle) = \langle \mathcal{I} \rangle P(\mathcal{I}) \qquad (2)$$

TABLE I: The topology of the shortest PO's of a fully connected graph with valency v are shown with the corresponding amplitude, Lyapunov exponent, and IPR.

t_p	p	A_p	$\Lambda_p(v \to \infty)$	$\mathcal{I}_p$
2		$(2/v - 1)^2$	$4/v$	$1/2$
3		$(2/v)^3$	$2 \ln v$	$1/6$
4		$(2/v)^2(2/v - 1)^2$	$\ln v$	$1/4$
		$(2/v)^4$	$2 \ln v$	$1/8$

indicating that the whole bulk of $\mathcal{P}(\mathcal{I})$ is effectively determined by the least unstable orbits (Fig. 1c).

With all this evidence for their prominent role in wavefunction localization, one clearly expects to see strong scarring on the period 2 orbits [17]. Such states would essentially be concentrated on two directed bonds and give rise to $\mathcal{I} \sim 1/2$. However, in this region $\mathcal{P}(\mathcal{I})$ is negligible. *The shortest and least unstable orbits of our system produce no visible scars.* Note that the same applies also to the value $\mathcal{I} = 1/4$ expected from the V-shaped orbits of Table I. In fact $\mathcal{P}(\mathcal{I})$ has an appreciable value only for $\mathcal{I} \leq 1/6$ (Fig. 1b). The position of this cutoff precisely coincides with the IPR expected for states which are scarred by triangular orbits. They occupy six directed bonds since, due to time-reversal symmetry, scarring on a PO and its reversed must coincide. Indeed a closer inspection shows that the vast majority of states at $\mathcal{I} \approx 1/6$ look like the example shown in Fig. 1a (right). Of course the step at $\mathcal{I} = 1/6$, which is present for any graph size V, is incompatible with the scaling of $P(\mathcal{I})$ mentioned above and indeed this relation breaks down in the tails at the expected points (inset of Fig. 1c). We conclude that *visible scars on short unstable orbits can strongly modify the tails of the IPR distribution* even beyond the known predictions for the influence of short PO's on wavefunction localization.

In the rest of the paper we will formulate a theory which explains the above observations. To this end we must be more explicit concerning the dynamics on the graph. We consider particles with fixed wavenumber k, propagating on the bonds and scattering at the vertices. During the free propagation on a directed bond the wavefunction accumulates a phase kL_{ij}, where $L_{ij} = L_{ji}$ denotes the length of the corresponding bond. At the vertices current conservation and continuity of the wave function are required. These boundary conditions can be translated into vertex scattering matrices, which describe a unitary transformation from v_i incoming to v_i outgoing waves at each vertex. Without loss of generality we restrict the presentation to the simplest case of *Neumann* boundary conditions [14], where the scattering matrix of

vertex i is

$$\sigma_{j,j'}^{(i)} = 2/v_i - \delta_{jj'} \,. \tag{3}$$

We can now combine the free propagation and the vertex scattering into a $2B \times 2B$ operator, the bond-scattering matrix S [14], which acts on the amplitudes a_d associated with the directed bonds. The matrix element

$$S_{m \to n, i \to j} = \delta_{mj}\,(2/v_j - \delta_{in})\,\mathrm{e}^{\mathrm{i}kL_{ij}} \tag{4}$$

describes a transition from the directed bond $d = [i \to j]$ to $d' = [m \to n]$. We interpret S as quantum time-evolution operator on the graph. $(S^t)_{d'd}$ is the complex probability amplitude to be after $t = 0, 1, \dots$ time steps on the directed bond d' if the initial state was on d. In particular, $|(S^t)_{dd}|^2$ is the quantum RP shown in Fig. 1b. $(S^t)_{dd} = \sum_p A_p \mathrm{e}^{\mathrm{i}kL_p}$ is expanded as a sum over all PO's of period t starting at d. Here L_p is the total length of orbit p. Assuming for simplicity $v_j \equiv v$ throughout the graph, we express the amplitude A_p by the number r_p of reflections along p, $A_p = (2/v)^{t-r_p}(2/v-1)^{r_p}$ (cf Table I). The classical RP is obtained by summing, instead of the amplitudes, the probabilities $M_p = |A_p|^2$. As $M_p < 1$, the probability to follow the PO decreases exponentially with time and the orbit is unstable. Hence one defines the *Lyapunov exponent* of a PO p on a graph by

$$\Lambda_p = -t_p^{-1} \ln M_p \,. \tag{5}$$

Let us now come back to the problem of scarring and investigate the conditions under which we can construct *perfect scars* on the graph, i. e. eigenstates $S|a\rangle = \mathrm{e}^{\mathrm{i}\lambda}|a\rangle$ which have the property that they have non-zero amplitude only on a PO p and vanish on all other bonds. Consider an arbitrary vertex j on p and let $D_{j,p}^{(\pm)}$ be the set of directed bonds which are leaving/approaching j and belong to p. Similarly let $\widehat{D}_{j,p}^{(\pm)}$ be the set of bonds *not* belonging to p. By construction, the amplitude of $|a\rangle$ on these latter bonds vanishes, i. e. all waves arriving on the bonds $D_{j,p}^{(-)}$ and transmitted across the vertex to a bond in $\widehat{D}_{j,p}^{(+)}$ cancel each other

$$0 = \sum_{d'} S_{dd'} a_{d'} = \frac{2}{v_j} \sum_{d' \in D_{j,p}^{(-)}} \mathrm{e}^{\mathrm{i}kL_{d'}}\,a_{d'} \quad (d \in \widehat{D}_{j,p}^{(+)}). \tag{6}$$

This equation has an important consequence: a perfect scar cannot live on a single bond attached to j because there would be no way to cancel the transmitted wave. An exception are only vertices with valency $v_j = 1$, for which $\widehat{D}_{j,p}^{(\pm)}$ is empty. Formally a necessary *condition for scarring orbits* p is

$$v_{j,p} \geq 2 - \delta_{v_j,1} \qquad (\forall j \in p) \tag{7}$$

where $v_{j,p}$ denotes the number of bonds attached to j and belonging to p. Eq. (7) excludes, in particular, perfect scars on the period-two orbits. Applying the same

reasoning that lead to Eq. (6) now to the bonds $D_{j,p}^{(+)}$ and making use of Eq. (3) we get

$$\mathrm{e}^{\mathrm{i}\lambda}\,a_d = -\mathrm{e}^{\mathrm{i}kL_d}\,a_{\hat{d}} \qquad (d \in D_{j,p}^{(+)})\,, \tag{8}$$

which relates the amplitude on a directed bond $d \in p$ to the amplitude on the reversed bond $\hat{d} \in \hat{p}$. This means that the same states are scarred on p and $\hat{p}$, as expected from time-reversal symmetry. Substituting $d \Rightarrow \hat{d}$ we get $\mathrm{e}^{\mathrm{i}\lambda}\,a_{\hat{d}} = -\mathrm{e}^{\mathrm{i}kL_d}\,a_d$ which together with Eq. (8) implies

$$(kL_d - \lambda)\,\mathrm{mod}\,\pi = 0 \qquad \forall\, d \in p \tag{9}$$

with arbitrary λ [18]. Eq. (9) is a necessary and sufficient condition for the energies of perfect scars. It is reminiscent of a simple Bohr-Sommerfeld quantization condition $kL_p = 2n\pi + \lambda$, as it applies, e. g., to strong scars in billiards. However, there is an important difference: not only does Eq. (9) require quantization of the total action kL_p of the scarred orbit, it also implies action quantization on all the visited bonds d. This stronger condition can only be met if the lengths of all bonds on p are rationally related. As in general the bond lengths are incommensurate *there are no perfect scars for generic graphs.*

Nevertheless, for incommensurate bond lengths Eq. (9) can be approximated with any given precision and then visible scars are expected. A natural measure for the quality of a scarred state $|a\rangle$ is the total probability $\delta_p = \sum_{d \notin p} |a_d|^2$ to find this state away from the scarring orbit ($\delta_p = 0$ corresponds to a perfect scar). We will derive the probability density of strong visible scars $\mathcal{P}(\delta_p \to 0)$. We represent the bond-scattering matrix S as perturbation of a matrix S_0 which has a perfect scar on p, i.e.

$$S = \mathrm{e}^{+\mathrm{i}\varepsilon\Phi}\,S_0 \approx (1 + \mathrm{i}\varepsilon\Phi)S_0\,. \tag{10}$$

The deviations from exact quantization for the individual bonds $d \in p$ have been combined into a diagonal matrix Φ with $\varepsilon\Phi_{dd} = (kL_d - \lambda)\,\mathrm{mod}\,\pi$ for $d \in p, \hat{p}$ and $\Phi_{dd} = 0$ otherwise. The strength of the perturbation is given by $\varepsilon_p = \min_\lambda \max_{d \in p} |(kL_d - \lambda)\,\mathrm{mod}\,\pi|$. For a PO covering N undirected bonds of the graph N bond phases $kL_d \,\mathrm{mod}\,\pi$ must approximately coincide. Upon variation of k, they are independent and uniformly distributed random numbers in $[-\pi, +\pi]$. Therefore the probability density of a small perturbation is $p(\varepsilon \to 0) \sim \varepsilon^{N-2}$. From first order perturbation theory we have

$$\delta = \varepsilon^2 \sum_{d \notin p} \left| \sum_{m \neq n} \frac{\langle a_m^{(0)}|\hat{\Phi}|a_n^{(0)}\rangle \langle d|a_m^{(0)}\rangle}{1 - \mathrm{e}^{\mathrm{i}(\lambda_m^{(0)} - \lambda_n^{(0)})}} \right|^2, \tag{11}$$

where $\lambda_m^{(0)}$, $|a_m^{(0)}\rangle$ are eigenphases and eigenvectors of S_0, including the perfect scar $|a_n^{(0)}\rangle$. The quantity $x = \delta/\varepsilon^2$ is distributed with some probability density $\tilde{p}(x)$ that is independent on ε. Consequently we have $p(\delta|\varepsilon) =$
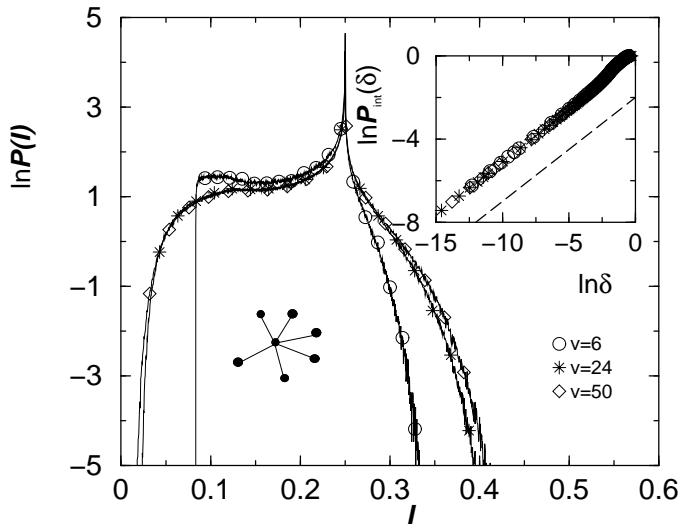
FIG. 2: $\mathcal{P}(\mathcal{I})$ for star-graphs of various valencies (inset a star-graph with $v = 6$). In the upper inset we report the integrated distribution $\mathcal{P}_{\mathrm{int}}(\delta) = \int_0^\delta d\delta' P(\delta')$ in a double-logarithmic plot. The dashed line has slope 0.5 which corresponds to the theoretical prediction Eq. (12).

$\varepsilon^{-2}\,\tilde{p}(\delta/\varepsilon^2)$. We can now use $\mathcal{P}(\delta) = \int d\varepsilon\, p(\delta|\varepsilon)\, p(\varepsilon)$ together with $p(\varepsilon \to 0) \sim \varepsilon^{N-2}$ to deduce

$$\mathcal{P}^{(N)}(\delta) = C\,\delta^{(N-3)/2} \qquad (\delta \to 0)\,. \qquad (12)$$

Here $C = \int dx\, x^{-(N-1)/2}\, \tilde{p}(x)$ is a constant which depends on the size and topology of the graph. Note that, according to Eq. (11), x is a sum of $B - N$ independent non-negative terms $x = \sum_{d \notin p} |x_d|^2$. Hence, $\tilde{p}(x)$ vanishes as x^{B-N} for $x \to 0$ and as a consequence the above integral C exists.

For fully connected graphs, triangles are the shortest orbits compatible with Eq. (7) and we have $\mathcal{P}^{(3)}(\delta \to 0) = C$, i. e. the probability of scarring does not depend on the required quality of the scar. This is in excellent agreement with numerical results (Fig. 1e) and compatible with the step-like cutoff in $\mathcal{P}(\mathcal{I})$ [19]. In a similar way we can describe the statistics of scars on other orbits. For example, according to Eq. (7), the square-shaped orbits of Table I can support scars and we did observe such states. However, Eq. (12) gives $\mathcal{P}^{(4)}(\delta \to 0) \sim \delta^{1/2}$, i. e. the probability of strong square scars is much smaller than for triangles and consequently they leave no distinct trace in $\mathcal{P}(\mathcal{I})$.

In contrast to fully connected graphs, Eq. (7) allows in star graphs scarring on the V-shaped orbits of Table I, because the outer vertices have valency 1. Applying Eq. (12) in this case we get $\mathcal{P}(\delta \to 0) \sim \delta^{-1/2}$, i. e. scarring is strongly enhanced. As a consequence $\mathcal{P}(\mathcal{I})$ is here totally dominated by scars, showing a strong maximum at $\mathcal{I} = 0.25$ (Fig. 2). It would be very interesting to relate this fact to spectral statistics, which for star graphs corresponds to pseudo-integrable instead of chaotic classical dynamics [16].

Discussions with E. J. Heller, S. Fishman and U. Smilansky are gratefully acknowledged. T. K. acknowledges support by a Grant from the GIF, the German-Israeli Foundation for Scientific Research and Development.

[1] E. J. Heller, Phys. Rev. Lett. **53**, 1515 (1984).
[2] L. Kaplan and E. J. Heller, Ann. Phys. **264**, 171 (1998). L. Kaplan, Phys. Rev. Lett. **80**, 2582 (1998).
[3] E. B. Bogomolny, Physica D **31**, 169 (1988). R. L. Waterland et al., Phys. Rev. Lett. **61**, 2733 (1988). D. Wintgen and A. Hönig, Phys. Rev. Lett. **63**, 1467 (1989). B. Eckhardt, G. Hose, and E. Pollak, Phys. Rev. A **39**, 3776 (1989). M. V. Berry, Proc. R. Soc. A **423**, 219 (1989). S. Tomsovic and E. J. Heller, Phys. Rev. Lett. **70**, 1405 (1993). D. Klakow and U. Smilansky, J. Phys. A **29**, 3213 (1996). F. Faure, S. Nonnenmacher, S. De Bievre, preprint nlin.CD/0207060.
[4] O. Agam and S. Fishman, Phys. Rev. Lett. **73**, 806 (1994). S. Fishman, B. Georgeot, and R. E. Prange, J. Phys. A **29**, 919 (1996).
[5] L. Kaplan, Phys. Rev. E **6403**, 036225 (2001).
[6] S. Sridhar, Phys. Rev. Lett. **67**, 785 (1991). J. Stein and H. J. Stöckmann, Phys. Rev. Lett. **68**, 2867 (1992).
[7] P. B. Wilkinson et al., Nature **380**, 608 (1996).
[8] J. P. Bird, R. Akis, and D. K. Ferry, Phys. Scr. **T90**, 50 (2001).
[9] A. Kudrolli, M. C. Abraham, and J. P. Gollub, Phys. Rev. E **6302**, 026208 (2001).
[10] C. Gmachl et al., Opt. Lett. **27**, 824 (2002).
[11] M. L. Mehta, *Random Matrices* (Academic Press, New York, 1991).
[12] P. Kuchment, Waves in Random Media **12**, R1 (2002). P. Kuchment, ed., *Waves in Random Media: Special Issue on Quantum Graphs* (IOP, 2003).
[13] *Proceedings of the 33rd ACM Annual Symposium on the Theory of Computing* (ACM Press, 2001).
[14] T. Kottos and U. Smilansky, Phys. Rev. Lett. **79**, 4794 (1997).
[15] T. Kottos and U. Smilansky, Ann. Phys. **274**, 76 (1999); Phys. Rev. Lett. **85**, 968 (2000); J. Phys. A (2003). H. Schanz and U. Smilansky, Phys. Rev. Lett. **84**, 1427 (2000). J. Desbois, J. Phys. A **33**, L63 (2000). G. Tanner, J. Phys. A **33**, 3567 (2000); J. Phys. A **34**, 8485 (2001). F. Barra and P. Gaspard, J. Stat. Phys. **101**, 283 (2000). G. Berkolaiko and J. P. Keating, J. Phys. A **32**, 7827 (1999). P. Pakonski, K. Zyczkowski, and M. Kus, J. Phys. A **34**, 9303 (2001). L. Hufnagel, R. Ketzmerick, and M. Weiss, Europhys. Lett. **54**, 703 (2001). G. Berkolaiko, H. Schanz, and R. S. Whitney, Phys. Rev. Lett. **88**, 104101 (2002). S. Gnutzmann et al., preprint cond-mat/0207388.
[16] G. Berkolaiko, E. B. Bogomolny, and J. P. Keating, J. Phys. A **34**, 335 (2001).
[17] Apparently this expectation is also supported by other scar theories which up to now have not been applied to graphs. For example, Agam and Fishman [4] predicted the positions of visible scars by a PO sum in which the orbits are weighed according to their stability.

[18] For $\lambda = 0$ the scarred states satisfy the secular equation for graphs [14]. We have checked that our results remain valid in this special case.

[19] Strictly speaking, δ gives only a lower bound for $\mathcal{I}$, $\mathcal{I} \geq 1/6 - \delta/3$, such that the step at $\mathcal{I} = 1/6$ is slightly smoothed. This is beyond the resolution of Fig. 1b).